2021 43rd Annual International Conference of the
IEEE Engineering in Medicine & Biology Society (EMBC)
Oct 31 - Nov 4, 2021. Virtual Conference

Neuromorphic Instantiation of Spiking Half-Centered Oscillator Models for Central Pattern Generation

Aditya Athota[1*], Blair Caccam[1*], Ryan Kochis[1*], Arjun Ray[1*],
Gert Cauwenberghs[1,2], Frédéric D. Broccard[2]

***Abstract*— In both invertebrate and vertebrate animals, small networks called central pattern generators (CPGs) form the building blocks of the neuronal circuits involved in locomotion. Most CPGs contain a simple half-center oscillator (HCO) motif which consists of two neurons, or populations of neurons, connected by reciprocal inhibition. CPGs and HCOs are well characterized neuronal networks and have been extensively modeled at different levels of abstraction. In the past two decades, hardware implementation of spiking CPG and HCO models in neuromorphic hardware has opened up new applications in mobile robotics, computational neuroscience, and neuroprosthetics. Despite their relative simplicity, the parameter space of GPG and HCO models can become exhaustive when considering various neuron models and network topologies. Motivated by computational work in neuroscience that used a brute-force approach to generate a large database of millions of simulations of the heartbeat HCO of the leech, we have started to build a database of spiking chains of multiple HCOs for different neuron model types and network topologies. Here we present preliminary results using the Izhikevich and Morris-Lecar neuron models for single and pairs of HCOs with different inter-HCO coupling schemes.**

I. Introduction

Central pattern generators (CPGs) are small neuronal circuits that can produce rhythmic patterns of activity [1]. The rhythmic activity results from the intrinsic properties of the component neurons and their synaptic interactions within a CPG, and underlies many of the adaptive rhythmic movements such as breathing, chewing, and digesting. In both invertebrate and vertebrate animals, CPGs also form the building blocks of the neuronal circuits involved in locomotion [2]. Experimental and computational work has identified and characterized the half-center oscillator (HCO) as a circuit building block of most invertebrate and vertebrate CPGs [3]. The HCO is composed of two neurons, or populations of identical neurons, connected by reciprocal inhibition (Fig. 1a). In segmented animals such as the leech, the stick insect, and the lamprey, a chain of multiple HCOs (Fig. 1b) regulates the activity and coordination of the individual segments [4]–[6]. In vertebrates, the network architecture of CPGs consist of one or several HCO motifs connected to additional neurons.

Computational modeling has been instrumental in the study of CPGs and HCOs, resulting in a plethora of computational models with different levels of abstraction ranging from detailed biophysical models of individual neurons [7] to mathematical models of coupled nonlinear oscillators to study population dynamics [8], [9]. Despite their relative simplicity, spiking models of CPGs and HCOs are of particular interest as their implementation in neuromorphic hardware has opened up new applications in mobile robotics [10], [11], computational neuroscience [12], and neuroprosthetics [13], [14]. Single HCO motifs have been implemented in custom analog neuromorphic VLSI hardware [15]–[18], and chains of HCOs have been implemented on FPGA boards and the SpiNNaker platform for the control of a hexapod robot [19]. A more complicated CPG architecture of ten neurons, including two pairs of HCOs implemented on FPGA boards, was used in a neuroprosthesis prototype in rats [13], and a chain of the same CPG models was implemented for the locomotion control of a snake robot [20].

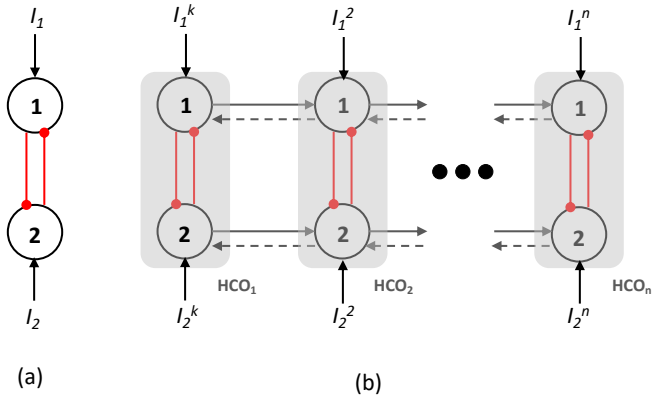

Fig. 1. Schematic representation of a single HCO with reciprocal inhibition (a) and a chain of n HCO motifs (b). Red lines correspond to inhibitory connections. Connections between two adjacent HCOs (dark gray arrows) can be excitatory or inhibitory. Dashed arrows represent feedback connections.

Depending on the level of abstraction of the individual neurons and the different network topologies studied, the parameter space of these HCO and CPG models can become very large. In computational neuroscience, the systematic exploration of the parameter space of biophysically detailed individual neuron models [21] and HCO models [22], [23] was carried out to built two large databases with millions of simulations with different parameter combinations. These database were created mainly for neuroscientists to shed light on how intrinsic membrane conductances and synaptic interactions give rise to specific network activity patterns. Although spiking models of HCOs and chains of HCOs

[1]Department of Bioengineering, Jacobs School of Engineering, and [2]Institute for Neural Computation, UC San Diego, La Jolla, CA 92093, USA.
*Contributed equally.

have been implemented with the Izhikevich [24] and the Morris-Lecar [25] neuron models [20], [24]–[26], there is currently no database of chains of multiple spiking HCO models available to inform their design and implementation in neuromorphic hardware. Our long-term goal is to build such a database by simulating chains of multiple HCO models for different types of bursting neuron models and network connectivity. Here we present results for pairs of HCOs constructed with two types of neuron models and various coupling schemes.

II. Methods

Single HCOs and chains of multiple HCOs were constructed with two types of spiking neuron models that reproduce the bursting behavior observed in animal HCOs: the Izhikevich and Morris-Lecar neuron models. Moreover, both of these neuron models have been implemented in neuromorphic hardware HCOs models used in robotics [19], [20]. Each neuron of an isolated HCO received an external input current and an inhibitory connection from the other neuron (Fig. 1a).

A. Neural models

The Izhikevich neuron model [27] is defined by the following system of coupled differential equations:

$$v' = 0.04v^2 + 5v + 140 - u + I \tag{1}$$

$$u' = a(bv - u) \tag{2}$$

with the reset condition

$$\text{if } V \geq 30 \text{ mV}, \text{then} \begin{cases} v \leftarrow c \\ u \leftarrow u + d \end{cases} \tag{3}$$

where *u* and *v* are dimensionless variables, and *a*, *b*, *c* and *d* are dimensionless parameters. The variable *v* corresponds to the membrane potential of the neuron and *u* correponds to a membrane recovery variable. The parameter *a* represents the rate of recovery of *u*, *b* is the sensitivity of the recovery of subthreshold fluctuations of the membrane potential, and *c* and *d* are the after-spike reset values of the *v* and *u* variables, respectively. The parameter *c* corresponds to the leak reverse potential. Different parameter combinations can reproduce different bursting behaviors with varying number of spikes per burst and inter-burst intervals.

The Morris-Lecar neuron model [28] is another system of coupled differential equations defined as:

$$C\frac{dV}{dt} = -g_L(V - V_L) - g_{Ca}m_\infty(V - V_{Ca}) - g_K w(V - V_K) + I \tag{4}$$

$$\frac{dw}{dt} = \lambda_w(V)(w_\infty(V) - w) \tag{5}$$

where g_L, g_{Ca}, g_K are the leak, calcium, and potassium conductances, and m_∞ and *w* are the gating variables for calcium and potassium, respectively. The voltage trace of this model does not represent individual spikes but rather the burst envelope.

B. Network topology and output patterns of activity

We explored isolated spiking HCO motif and chains of multiple HCOs with different coupling schemes. For chains of HCOs, we added a synaptic current to the voltage equations. A synaptic conductance with a single exponential decay was used for the simulations with the Izhikevich neuron model. For simulations with the Morris-Lecar neuron model, synapses were modeled as a sigmoidal function of the pre-synaptic voltage [26] and the corresponding synaptic current is given by:

$$I_{syn} = g_{syn}s_{ji}(V_j)(V_i - E_{syn}) \tag{6}$$

with

$$s_{ji}(V_j) = 0.5(1 + \tanh(\frac{V_j - \eta}{k})) \tag{7}$$

where i and j refer to the pre-synaptic and post-synaptic neuron, respectively, η is the synaptic threshold, and k the synaptic gain.

For pairs of coupled HCOs, we considered purely feedforward excitatory connections and mixed excitatory feedforward and feedback connections. Feedforward and mixed feedforward/feedback connections could be between the same neuron of both HCOs or between different neurons of each HCO (cross-connections), e.g. excitatory connection between neuron 1 of HCO_1 and neuron 2 of HCO_2.

The spiking activity of a given HCO was classified in four distinct types: *silent, asymmetric, spiking, and bursting*. A HCO was classified as silent when none of the two neurons spiked, or as asymmetric when only one of the neuron spiked. When both neurons fired, we distinguished between spiking and bursting patterns of activity.

C. Simulations and database organization

Simulations of spiking HCOs with both types of neuron models were carried using a brute-force approach in which we systematically explored the parameter space by varying each individual parameter. The differential equations of both neuron types were integrated by using the 4th order Runge-Kutta method with a time step of 0.1 ms. Custom Matlab (The Math Works, Inc.) code was run on a desktop computer and on multicore processors through the Neuroscience Gateway (NSG) portal [29]. After changing an individual parameter, each simulation was run for 5 seconds to allow the model to reach a stable activity. The simulations were then continued for another 40 seconds during which we recorded the spiking and bursting activity of each individual neuron. Results from the simulations were stored in a hierarchical folder structure. For each non-silent HCO, we computed its period, duty cycle, and phase between the two neurons. All parameters were varied across 0%, 25%, 50%, 75%, 100%, 150%, and 200% of their canonical values. The time constant of the single exponential inhibitory synapse in the Izhikevich neuron model was varied over across the values 20, 30, 40, 50, and 60 ms. The leak reverse potential in the Morris-Lecar neuron model was varied across the values -70, -65, -60, and -55 mV. The external input current was varied across

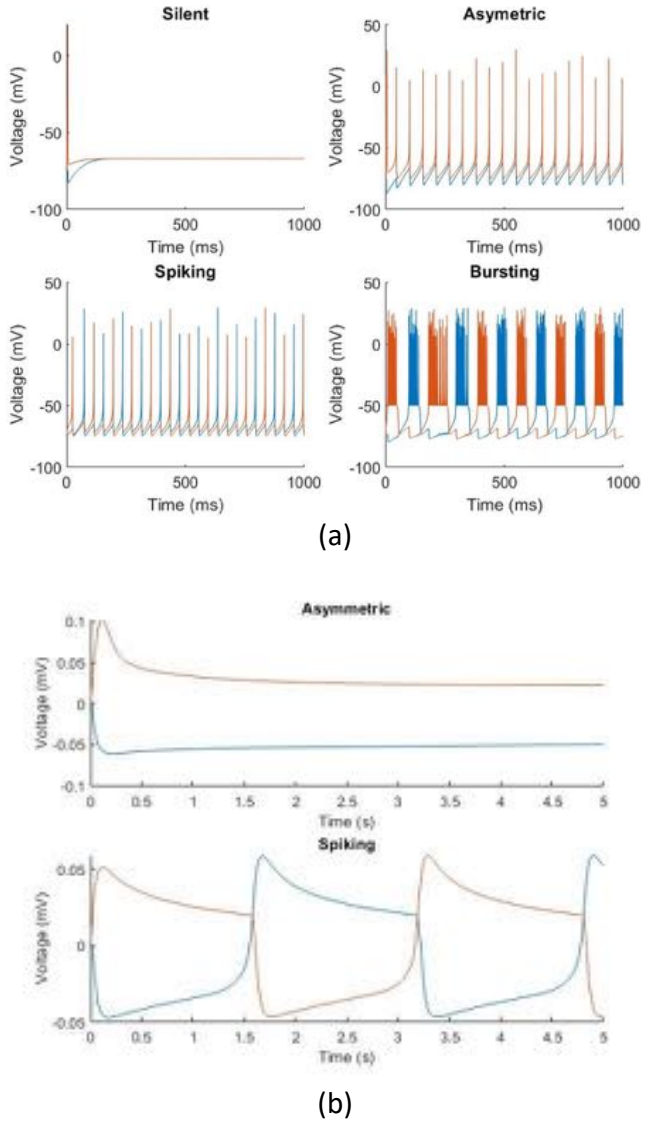

Fig. 2. Spiking behavior of two neurons of a single HCO motif for the Izhikevich (a) and Morris-Lecar (b) neuron models. In (a), the parameter values for the *silent* mode are: I=2, a=0.02, b=0.2, c=-65 mV, d=8, I_{syn}=8, τ_{syn} = 40ms; for the *spiking* mode, same as silent except I=8; for the *asymmetric* mode, same as spiking except I_{syn}=18; for the *bursting* mode, same as spiking, except I=5, c=-50 mV, d=0.5. In (b), the parameter values for the *spiking* mode are: I=0.8 μA, g_L=5 μS, g_{Ca}=15 μS, g_K=20 μS, g_{syn}=10 μS, E_L=-50 mV; for the *asymmetric* mode, same as spiking, except g_K=10 μS and g_{syn}=5 μS. The voltage traces of different neurons are indicated in different colors.

the values 0.4, 0.6, 0.8 and 1 μA for three different levels of Gaussian noise (0, 1, and 2 standard deviation).

III. Results

HCOs with different patterns of spiking activity are shown in Figure 2 for both types of neuron models. Each HCO was constructed with a different set of parameters.

Dimensional stacking [30] was used for the data visualization of all simulations for a given HCO model. Dimensional stacking provides a quick way to visually determine regions of the parameter space correspoonding to silent, and therefore non-functional, HCOs with no spike and zero phase. The mean period of a single HCO motif composed of two Morris-Lecar neurons for all parameters values is shown in Figure 3. In that plot, the values of the external current I, leak conductance g_L, and calcium conductance g_{Ca} are represented on the x axis, while the values of the potassium conductance g_K, synaptic conductance g_{syn}, and reverse potential E_L are on the y axis. Each parameter value corresponds to a bin which is further subdivided to accommodate the representation of the other parameters. In these simulations, the external current was identical for both neurons and contained no noise. The synaptic conductance was varied across the values 5, 10, 15, and 20 ms. The synaptic reverse potential was not varied and was kept at -20 mV in order to facilitate the data visualization.

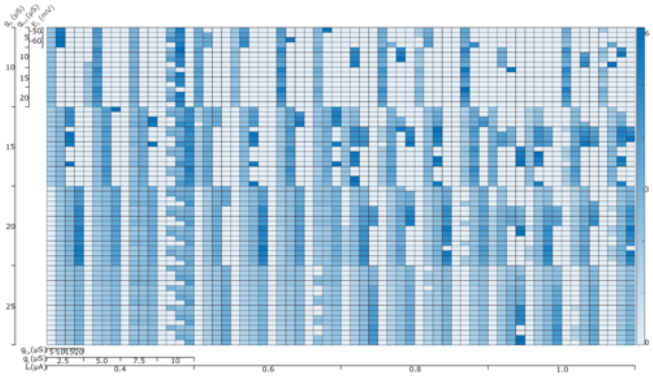

Fig. 3. Dimensional stacking of all 4,096 simulations for a single HCO motif with the Morris-Lecar neuron model. The period of each HCO is color-coded according to the colormap on the right. Darker shades of blue correspond to higher periods. Each bin on the x and y axis corresponds to a range of values for each parameter. The calcium conductance g_{Ca}, leak conductance g_L, and external current I_μ values are represented on the x axis. The external current has no noise and the different noise levels are not shown. The leak reverse potential E_L, synaptic conductance g_{syn}, and potassium conductance g_K values are represented on the y axis.

For pairs of coupled HCOs, we investigated the influence of the coupling scheme between adjacent HCO motifs on the number of spikes per burst fired by each individual HCO (Figure 4) composed of Izhikevich neurons. In these simulations, feedforward connections from HCO_1 to HCO_2 were purely excitatory, and feedback connections were either excitatory (exc.) or inhibitory (inh.).

IV. Conclusion

In this work, we have presented preliminary results toward the creation of a database of spiking HCO networks composed of one or multiple HCO motifs, and using different types of busrting neuron models. Simulations were carried out through the freely available high-performance cloud computing resources of the NSG portal. This database is envisioned as a resource to help and facilitate the design and implementation of spiking HCO and CPG network models in neuromorphic hardware and FPGA boards. Once completed, this database will be made publicly available.

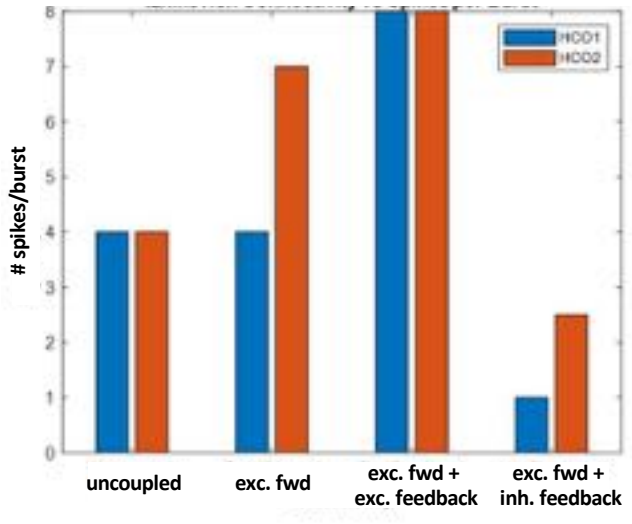

Fig. 4. Effect of the coupling scheme between pairs of HCOs connected on the number of spikes per burst for each individual HCO.

ACKNOWLEDGMENT

The authors thank members of the Neuroscience Gateway (NSG) portal at the San Diego Supercomputer Center (SDSC), including Kenneth Yoshimoto, for assistance with the numerical simulations.

REFERENCES

[1] F. Delcomyn, "Neural basis for rhythmic behaviour in animals," *Science*, 210, 492–498, 1980.

[2] K.G. Pearson, "Common principles of motor control in vertebrates and invertebrates," *Annual Review of Neuroscience*, 16(1), 265-297, 1993.

[3] E. Marder and D. Bucher, "Central pattern generators and the control of rhythmic movements," *Current Biology*, 11(23), R986-R996, 2001.

[4] K.A. Sigvardt and T.L. Williams, "Effects of local oscillator frequency on intersegmental coordination in the lamprey locomotor CPG: theory and experiment," *Journal of Neurophysiology*, 76(6), 4094-4103, 1996.

[5] K.J. Muller, J.G. Nicholls, and G.S. Stent, *Neurobiology of the Leech*. Cold Spring Harbor Laboratory, 1981.

[6] U. B$\acute{}$assler, U.and A. B$\acute{}$uschges," Pattern generation for stick insect walking movements—multisensory control of a locomotor program," *Brain Research Reviews*, 27(1), 65-88, 1998.

[7] S. Daun–Gruhn, and T.I. Tóth, "An inter-segmental network model and its use in elucidating gait-switches in the stick insect," *Journal of Computational Neuroscience*, 31(1), 43-60, 2011.

[8] T.L. Williams, "Phase coupling in simulated chains of coupled oscillators representing the lamprey spinal cord," *Neural Computation*, 4(4), 546-558, 1992.

[9] J.J. Collins and I. Stewart, "Hexapodal gaits and coupled nonlinear oscillator models," *Biological Cybernetics*, 68(4), 287-298, 1993.

[10] M.A. Lewis, R. Etienne-Cummings, A.H. Cohen and M. Hartmann, "Toward biomorphic control using custom aVLSI CPG chips," in *Proceedings 2000 ICRA. Millennium conference. IEEE international conference on robotics and automation. Symposia proceedings (Cat. No. 00CH37065)*, 1, 494-500, 2000.

[11] A.J. Ijspeert, "Central pattern generators for locomotion control in animals and robots: A review," *Neural Networks*, 21, 642-653, 2008.

[12] R. Jung, E.J. Brauer and J.J. Abbas,"Real-time interaction between a neuromorphic electronic circuit and the spinal cord," *IEEE Transactions on Neural Systems and Rehabilitation Engineering*, 9(3), 319-326, 2001.

[13] S. Joucla, M. Ambroise, T. Levi, T. Lafon, P. Chauvet, S. Saïghi, Y. Bornat, N. Lewis, S. Renaud and B. Yvert, "Generation of locomotor-like activity in the isolated rat spinal cord using intraspinal electrical microstimulation driven by a digital neuromorphic CPG," *Frontiers in Neuroscience* 10, 67, 2016.

[14] F.D. Broccard, S.Joshi, J. Wang, and G. Cauwenberghs, "Neuromorphic neural interfaces: from neurophysiological inspiration to biohybrid coupling with nervous systems" *Journal of Neural Engineering*, 14(4), 041002, 2017.

[15] G.S. Cymbalyuk, G.N. Patel, R.L. Calabrese, S.P. DeWeerth and A.H. Cohen, "Modeling alternation to synchrony with inhibitory coupling: A neuromorphic VLSI approach," *Neural Computation*, 12(10), 2259-2278, 2000.

[16] M.F. Simoni and S.P. DeWeerth, "Two-dimensional variation of bursting properties in a silicon-neuron half-center oscillator," *IEEE Transactions on Neural Systems and Rehabilitation Engineering*, 14(3), 281-289, 2006.

[17] T. Yu and G. Cauwenberghs, "Analog VLSI biophysical neurons and synapses with programmable membrane channel kinetics," *IEEE Transactions on Biomedical Circuits and Systems*, 4(3), 139-148, 2010.

[18] K. Nakada, T. Tetsuya, T. Hirose, and Y. Amemiya, "Analog CMOS implementation of a neuromorphic oscillator with current-mode low-pass filters," in *IEEE International Symposium on Circuits and Systems*, pp. 1923-1926, 2005.

[19] D. Gutierrez-Galan, J.P. Dominguez-Morales, F. Perez-Peña, A. Jimenez-Fernandez, and A. Linares-Barranco, "NeuroPod: a real-time neuromorphic spiking CPG applied to robotics," *Neurocomputing*, 381, 10-19, 2020.

[20] D. Blanchard, K. Aihara and T. Levi,"Snake robot controlled by biomimetic CPGs", *Journal of Robotics, Networking and Artificial Life*, 5(4), 253-256, 2019.

[21] A.A. Prinz, C.P. Billimoria, and E. Marder, "Alternative to hand-tuning conductance-based models: construction and analysis of databases of model neurons," *Journal of Neurophysiology*, 90(6), 3998-4015, 2003.

[22] A. Doloc-Mihu and R.L. Calabrese, "A database of computational models of a half-center oscillator for analyzing how neuronal parameters influence network activity," *Journal of Biological Physics*, 37(3), 263-283, 2011.

[23] A. Doloc-Mihu and R.L. Calabrese, "Analysis of family structures reveals robustness or sensitivity of bursting activity to parameter variations in a half-center oscillator (HCO) model," *Eneuro*, 3(4), 2016.

[24] P. Tolmachev, R.R. Dhingra, M. Pauley, M. Dutschmann, and J.H. Manton, "Modeling the respiratory Central Pattern Generator with resonate-and-fire Izhikevich-Neurons," in *International Conference on Neural Information Processing*, pp. 603-615, 2018.

[25] Z. Yuand P.J. Thomas, "Dynamical consequences of sensory feedback in a half-center oscillator coupled to a simple motor system." *Biological Cybernetics*, 1-26, 2021.

[26] C. Zhang and T.J. Lewis, "Robust phase-waves in chains of half-center oscillators," *Journal of Mathematical Biology*, 74, 1627-1656, 2017.

[27] E. Izhikevich, "Simple model of spiking neurons," *IEEE Transactions on Neural Networks*, 14(6), 1569-1572, 2003.

[28] C. Morris and H. Lecar , "Voltage oscillations in the barnacle giant muscle fiber," *Biophysical Journal*, 35, 193-213, 1981.

[29] S. Sivagnanam, A. Majumdar, K.Yoshimoto, V. Astakhov, A.E. Bandrowski, M.E. Martone and N.T. Carnevale," Introducing the Neuroscience Gateway," *IWSG* 993, 2013. https://www.nsgportal.org/

[30] J. LeBlanc, M.O. Ward and N. Wittels, "Exploring n-dimensional databases,", in *VIS '90: Proceedings of the 1st conference on Visualization '90*, 230–237, Los Alamitos, CA, USA, 1990. IEEE Computer-Society Press.